



**HAL**  
open science

## Low exposition to lithium prevents nephrogenic diabetes insipidus but not microcystic dilations of the collecting ducts in long-term rat model

Nahid Tabibzadeh, Mathieu Klein, Mélanie Try, Joël Poupon, Pascal Houillier, Christophe Klein, Lydie Cheval, Gilles Crambert, Samia Lasaad, Lucie Chevillard, et al.

### ► To cite this version:

Nahid Tabibzadeh, Mathieu Klein, Mélanie Try, Joël Poupon, Pascal Houillier, et al.. Low exposition to lithium prevents nephrogenic diabetes insipidus but not microcystic dilations of the collecting ducts in long-term rat model. *Archiv der Pharmazie / Chemistry in Life Sciences*, 2024, 357 (8), 10.1002/ardp.202400063 . hal-04728445

**HAL Id: hal-04728445**

**<https://hal.science/hal-04728445v1>**

Submitted on 10 Oct 2024

**HAL** is a multi-disciplinary open access archive for the deposit and dissemination of scientific research documents, whether they are published or not. The documents may come from teaching and research institutions in France or abroad, or from public or private research centers.

L'archive ouverte pluridisciplinaire **HAL**, est destinée au dépôt et à la diffusion de documents scientifiques de niveau recherche, publiés ou non, émanant des établissements d'enseignement et de recherche français ou étrangers, des laboratoires publics ou privés.

## **Low exposition to lithium prevents nephrogenic diabetes insipidus but not microcystic dilations of the collecting ducts in long-term rat model**

Nahid Tabibzadeh<sup>1,2\*#</sup>, Mathieu Klein<sup>3\*</sup>, Mélanie Try<sup>1,2\*</sup>, Joël Poupon<sup>4</sup>, Pascal Houillier<sup>1,2,5</sup>, Christophe Klein<sup>6</sup>, Lydie Cheval<sup>1,2</sup>, Gilles Crambert<sup>1,2</sup>, Samia Lasaad<sup>1,2</sup>, Lucie Chevillard<sup>3</sup>, Bruno Megarbane<sup>3,7#</sup>

1. Laboratoire de Physiologie Rénale et Tubulopathies, Centre de Recherche des Cordeliers, INSERM, Sorbonne Université, Université Paris Cité, Paris, France.

2. EMR 8228 Unité Métabolisme et Physiologie Rénale, CNRS, Paris, France.

3. Inserm UMRS-1144, Université Paris Cité, Paris, France

4. Department of Biological Toxicology, AP-HP, Lariboisière Hospital, University Paris VII, Paris, France

5. Assistance Publique-Hôpitaux de Paris, Hôpital Européen Georges Pompidou, Service de Physiologie, 20 rue Leblanc, 75015, Paris, France.

6. Centre d'Histologie, d'Imagerie et de Cytométrie (CHIC), Centre de Recherche des Cordeliers, INSERM, Sorbonne Université, Université de Paris, Paris, France

7. Department of Medical and Toxicological Critical Care, Lariboisière Hospital, Federation of Toxicology, APHP, Paris, France

\*Authors contributed equally to the present work.

# Correspondence: NT [nahid.tabibzadeh@inserm.fr](mailto:nahid.tabibzadeh@inserm.fr) (+33140257546) and BM [bruno.megarbane@aphp.fr](mailto:bruno.megarbane@aphp.fr) (+33149958442)

**Keywords:** Lithium – nephrotoxicity – diabetes insipidus – kidney microcysts

## Abstract

Lithium induces nephrogenic diabetes insipidus (NDI) and microcystic chronic kidney disease (CKD). As previous clinical studies suggest that NDI is dose-dependent and CKD is time-dependent, we investigated the effect of low exposition to lithium in a long-term experimental rat model. Rats were fed with a normal diet (control group), or with the addition of lithium (Li<sup>+</sup> group), or with lithium and amiloride (Li<sup>+</sup>/Ami group) during 6 months, allowing obtaining low plasma lithium concentrations ( $0.25\pm 0.06$  and  $0.43\pm 0.16$  mmol/l respectively). Exposition to low concentrations of plasma lithium levels prevented NDI but not microcystic dilations of kidney tubules, that were identified as collecting ducts (CD) on immunofluorescent staining. Both hypertrophy, characterized by an increase in the ratio of nuclei per tubular area, and microcystic dilations were observed. The ratio between principal cells and intercalated cells was higher in ~~dilated~~ microcystic than in hypertrophied tubules. There was no correlation between AQP2 mRNA levels and cellular remodeling of the CD. Additional amiloride treatment in the Li<sup>+</sup>/Ami group did not allow consistent morphometric and cellular composition changes compared to the Li<sup>+</sup> group. Low exposition to lithium prevented overt NDI but not microcystic dilations of the CD, with differential cellular composition in hypertrophied and ~~dilated~~ microcystic CDs, suggesting different underlying cellular mechanisms.

## Introduction

Lithium ( $\text{Li}^+$ ) is the first line treatment for bipolar disorder (1–3), but its high efficacy is counterbalanced by long-term adverse effects (4). Among them, renal adverse effects are the most significant and are divided into 2 entities, the nephrogenic diabetes insipidus (NDI) and the microcystic chronic kidney disease (CKD) (5,6).

Regarding Li-induced microcystic CKD, previous experimental studies have reported tubular dilations and microcysts, developing as soon as 1 month after Li initiation (7–9). Interstitial fibrosis and uremia have also been induced in long-term exposition models up to 6 months (7,10). Based on morphological analyses and lectin staining, distal tubules and/or collecting ducts have been indirectly identified as the potential origin of dilations and microcysts (7,11). However, no specific staining has been reported, and the exact cellular composition of these cysts is not established. In this respect, experimental data have shown collecting duct remodeling characterized by cellular proliferative signals and an increase in the ratio between type A intercalated cells and principal cells (12–14).

Li-induced NDI is characterized by early polyuria and polydipsia due to renal resistance to vasopressin secondary to a decrease in AQP2 apical membrane addressing and expression (15). Whether a mechanistic relationship exists between Li-induced NDI and CKD remains to be determined. Moreover, the relationship between cellular composition, microcystic tubular dilations and resistance to the action of vasopressin is yet to be demonstrated.

As a matter of fact, NDI develops shortly after Li initiation in humans as well as in experimental models (16), while CKD is inconstant and very slowly progressive (17). Recent clinical studies suggest differential determinants of Li-induced NDI and CKD. While Li daily dose is the main determinant of the former (18), Li treatment duration is reported to be independently associated with the latter (19).

Amiloride is a therapeutic strategy in Li-induced NDI, based on case series of patients treated with lithium (20,21). Amiloride is a specific blocker of the Epithelial Sodium Channel (ENaC), hence of Li entry in principal cells (22–24). Regarding Li-induced microcystic CKD, two studies



have shown a reduction in kidney fibrosis and tubular dilations in rats treated with Li during 6 months at therapeutic doses when amiloride was concomitantly administered (25,26).

Based on these findings, the objective of this study was to evaluate in a rat model the effect of Li under-exposition on NDI and microcystic tubular dilations, the potential relationship between them and the efficacy of amiloride to prevent both.

## Results

*Under-exposition to lithium resulted in no overt NDI but in microcystic dilations of the collecting ducts*

Plasma lithium concentrations in rats treated with Li alone (Li<sup>+</sup> group) were  $0.25 \pm 0.06$  mmol/l. The Li<sup>+</sup> group displayed non-significantly higher urine output and lower urine osmolality than control rats (**figure 1**). Urine concentration challenging tests (hydric restriction and desmopressin injection) did not reveal a significantly altered urine concentration ability in the Li<sup>+</sup> group at 3 and 6 months of treatment. After 6 months of treatment, plasma creatinine was not statistically different between the 2 groups, and no overt interstitial fibrosis was observed on histopathological assessment (**figure 2**). However, consistent and marked tubular morphological changes were observed in the Li<sup>+</sup> group, characterized by cortical and outer medullary microcystic tubular dilations, sometimes associated with intratubular casts. Semi-automated cortical tubular area measurement showed significantly higher tubular areas and minimal diameters in the Li<sup>+</sup> group compared to controls (**figure 2**).

*A differential cellular composition of collecting ducts was observed in dilated-microcystic and non-dilated-microcystic collecting ducts*

Dilated-Microcystic tubules stained for markers of principal (PC) and type A intercalated (AIC) cells, demonstrating that the tubular segment involved in these dilations-microcystic dilations were collecting ducts (CD) (**figure 3**). Morphometric analysis of these collecting duct showed an increase in the size of cells and in the number of nuclei per tubular area in Li-treated rats compared to control rats, suggestive of epithelial hypertrophy. This was equally observed in the cortex, the outer medulla and the inner medulla (**figure 4**). Hypertrophy was not associated with positive Ki67 staining of CD cells at 6 months (**figure 3**).

The analysis of the composition of CDs revealed a decrease in the ratio between PCs and AICs in the Li group in the cortex, the outer medulla and the inner medulla (**figure 4**). However, the cellular composition of dilated-microcystic CDs was different, lined with a majority of PCs, conversely to hypertrophied CDs (**figure 4**).

Long-term exposure to lithium has been demonstrated to induce remodeling of the collecting ducts, particularly in the inner medulla, characterized by the presence of pendrin-positive cells (27). Therefore, we assessed pendrin expression across various renal segments to determine whether low-dose exposure altered its expression pattern. Consistent with prior findings, we observed that pendrin expression was markedly higher in the cortex compared to the deepest segments, by at least a five-fold increase (28), with no significant differences observed within each segment between control and lithium-treated rats (figure 4)

*Despite no overt NDI, AQP2 expression decreased in Li-treated rats, with ~~weak-minor~~ correlation with cellular remodeling*

On qualitative assessment of immunofluorescent staining, no difference in the expression pattern of AQP2 was observed between the experimental groups (figure 3). AQP2 mRNA levels were analyzed in the cortex, the outer stripe of the outer medulla (OSOM), the inner stripe of the outer medulla (ISOM) and the inner medulla, showing that mRNA levels were significantly lower in Li-treated rats compared to controls in all these segments, despite the absence of significantly higher urine output, with a decreased AQP2 expression gradient in the Li<sup>+</sup> group (**figure 5**). There was no statistical correlation between cellular and morphometric quantifications of CDs and the level of AQP2 expression except a correlation between AQP2 expression and the PC/AIC ratio that was found only in the outer medulla ( $\rho=0.61$ ,  $p=0.03$ ).

*Amiloride treatment had no effect on microcystic dilations but decreased the type A intercalated/principal cells ratio within the ~~non-hypertrophied/dilated~~ portions of the collecting ducts*

Plasma lithium levels were  $0.43 \pm 0.16$  mmol/l in rats treated with lithium and amiloride (Li<sup>+</sup>/Ami group,  $p=0.01$  compared with rats in the Li<sup>+</sup> group). Rats treated with Li and amiloride did not differ from the Li<sup>+</sup> group in terms of urine output, urine osmolality and plasma creatinine, and urine concentration ability after challenging tests, but with a lower weight gain than the two other groups over the study period (figure 1). -Tubular area quantifications were also similar

between the Li<sup>+</sup> and the Li<sup>+</sup>/Ami group (**figure 2**). Increased number of nuclei per external area was prevented exclusively in the renal cortex of the Li<sup>+</sup>/Ami group, with no statistical difference in the outer or the inner medulla (**figure 3**). This observation was associated with a less extended decrease in the PC/AIC ratio compared to the Li<sup>+</sup> group (**figure 3**), and no difference in this ratio between ~~dilated-microcystic~~ et ~~non-dilated-hypertrophied~~ CDs (**figure 4**). Finally, the reduction in AQP2 mRNA expression ~~decrease~~ was more ~~important~~pronounced, though not reaching statistical significance throughout all the kidney segments in the Li<sup>+</sup>/Ami group compared to the Li<sup>+</sup> group (**figure 5**). Overall, amiloride did not prevent AQP2 transcription decrease after 6 months of lithium exposure.

## Discussion

Our study showed in a rat model of Li exposition that lower plasma lithium concentrations resulted in the no overt nephrogenic diabetes insipidus, but did not prevent morphological changes and cellular remodeling consisting in microcystic dilations and hypertrophy of the collecting ducts.

The usual standard target plasma lithium levels are 0.6-1 mmol/l. However, several clinical trials suggest clinical efficacy of lower doses in bipolar disorder, with lithium concentrations of 0.4 mmol/l (29). Our previous study evaluating vasopressin resistance and NDI in Li-treated patients showed that the main determinant of urine output was Li daily dose, directly affecting plasma lithium concentrations, independently of treatment duration (18). Our experimental findings in a model with low plasma concentrations are consistent with the clinical findings as, even though a significant decrease in AQP2 expression was observed, no significant change in urinary output, urine osmolality, or urine concentration ability was evidenced. Immunofluorescent staining of AQP2 showed no apparent decrease in fluorescence intensity between the groups allowing to identify PCs with this staining. This suggests a resistance to the action of vasopressin to a certain degree, that might be obvious during hydric restriction challenge.

Despite the absence of polyuria or major AQP2 expression decrease, morphological changes were observed. These morphological changes involved the CDs, as suggested by previous studies with no direct evidence to date (11,16). Two features coexisted in all the analyzed kidneys, namely CD hypertrophy, characterized by an increase in the number of cells per tubular area, and microcystic dilations, characterized by CD enlargement and cellular stretching. Interestingly, cellular composition was different in ~~dilated~~microcystic and hypertrophic CDs, with a majority of PCs in the former and a higher proportion of AICs in the latter. While Bissler *et al.* reported that cysts developed in a murine model of tuberous sclerosis complex originated from AICs (30,31), cysts in experimental models of autosomal polycystic kidney disease (ADPKD) consisted both of PCs and ICs, with a major role of PCs in cyst development (32,33). Of note, primary cilia dysfunction represents an essential promoter of

renal cysts in ADPKD as well as in various cystic kidney diseases (generically referred to as ciliopathies), and are only present in PCs within the CDs (34).

Cellular remodeling has been previously reported during lithium treatment as well as during acute kidney injury (12,35). In our study, no proliferation was seen after 6 months of Li<sup>+</sup> treatment as assessed by Ki67 staining. Cells also presumably remained differentiated, with no double positive cells found on immunofluorescent analysis (AQP2<sup>+</sup>/AE1<sup>+</sup>). In this regard, Trepiccione *et al.* demonstrated the presence of double-positive cells bearing markers of both PCs and of AICs after Li discontinuation in a murine model (36). These cells were particularly concentrated at the end of long-row distribution of AICs, suggestive of a trans-differentiation and/or recovery process inducing PCs following Li suspension. The existence, time course and mechanisms of a potential CD cell proliferation during Li therapy are still a matter of debate. While Christensen *et al.* have found proliferation among PCs (37), De Groot *et al.* reported a G2 arrest of the cell cycle in these cells and a shift towards a higher proportion of AIC, in accordance with our findings (13). This shift might be due to trans-differentiation of PC into AIC rather than proliferation, a mechanism that is likely mediated by Notch signaling inactivation (38). This trans-differentiation is not associated with cellular proliferation in physiological conditions as well as during acute kidney damage (35). Early events remain to be evaluated in our model in order to determine a potential trans-differentiation with or without proliferation signals. Interestingly, the remodeling phenomena were barely correlated with the decrease in AQP2 expression, whereas one could have hypothesized such a correlation based on the decrease in the proportion of PCs. Our findings rather suggest that Li effect on urine concentration and on cellular remodeling are uncoupled. Accordingly, our previous reports evaluating patients treated with Li for bipolar disorder showed differential determinants of Li-associated NDI and Li-associated kidney texture changes using kidney MRI radiomic analyses (18,39).

We did not evidence elevated plasma creatinine levels or renal interstitial fibrosis suggestive of a decrease in renal function after 6 months of treatment, whereas interstitial fibrosis was reported by Walker *et al.* (7) after the same duration of treatment with higher exposition to

lithium. It remains to be determined whether cellular remodeling is deleterious in the long term, but our results, put in the perspective of previous literature, suggest that lowering kidney exposition to Li might be nephroprotective in a certain extent.

Finally, we studied the effect of amiloride treatment in this experimental under-exposed model. We found no difference between the group without and the group with amiloride regarding urine concentration. AQP2 mRNA expression was even lower, although not significantly, in the Li<sup>+</sup>/Ami group. However, this should be interpreted with caution as plasma lithium concentrations were higher, though still at infra-therapeutic levels, than in the Li<sup>+</sup> group. This is likely attributable to angiotensin II-mediated stimulation of proximal tubular sodium (and lithium) reabsorption, which occurs secondary to the natriuretic effect of Amiloride (40). The lower weight gain observed in the Amiloride treated rats may be indicative of a relative reduction in extracellular volume due to natriuresis. These findings also align with those reported in a prior study by Bedford et al (41). As a monovalent cation Li enters tubular cells using the same transporters as sodium. As a specific ENaC blocker, amiloride has been proven to inhibit Li entry in PCs *in vitro* and *in vivo* (22). Conversely to our findings, Bedford *et al.* demonstrated improved urine concentration and increased AQP2 expression when Li-exposed rats were treated with amiloride (41). Small clinical trials have shown an increase in urine osmolality and urinary AQP2 excretion after treating patients with amiloride (20,21). In a long term (5 months) murine model of Li nephrotoxicity, Kalita-De Croft *et al.* also showed that amiloride prevented renal fibrosis (25), although altered tubular morphology and microcystic dilations were not prevented, consistently with our study. The disparity in Li exposition among studies could account for the differences in our findings. In our study, a mild effect of amiloride was observed on cellular remodeling, in particular in the renal cortex, with a lesser decrease in the PC/AIC ratio. This effect is in line with recent literature showing an important crosstalk between PCs and AICs, especially during acidosis (23,42–44).

Our study displays limitations. First, due to the long-term treatment study design and the animal facility space limitations, we lacked an experimental group with plasma lithium concentrations at the therapeutic ranges, that might further evaluate the potential effect of amiloride on

hypertrophy and microcysts development. We thus based our protocol on previous literature showing NDI, kidney fibrosis and uremia, and microcystic kidney disease in the long-term setting (7,8,25). Second, our study also lacked early timepoint assessments in order to evaluate the early biochemical and morphological changes induced by exposition to lower plasma lithium levels. In particular, the evaluation of cell cycle disruption by Ki67 staining at 6 months was insufficient, and assessments at earlier time points are necessary to contextualize our model within previous literature. Li triggers the activation of cell cycle pathways at very early stages following initiation (45). Further studies at therapeutic levels of lithium exposition with early timepoints of assessments would thus help better evaluate CD remodeling in this setting. Finally, our transcript analyses could not be complemented by protein analyses due to the unavailability of kidney tissue.

In conclusion, under-exposition of kidneys to lithium resulted in the prevention of overt nephrogenic diabetes insipidus although AQP2 expression was decreased, but did not prevent collecting duct hypertrophy and microcysts, with only minor effect of amiloride on cellular remodeling. Future studies are needed to better decipher the differential role of signaling pathways leading to hypertrophy and intercalated cell number increase on the one hand, and microcysts generated from principal cells on the other hand.



## Experimental

### *Animals*

All procedures were performed in accordance with the French animal care legislation, and were approved by the Ethics committee of the Université Paris Cité and by the French Ministry of Research (approval # 26674-2020020714451509). Wild-type male Sprague-Dawley rats (mean weight of 100-125 g, Janvier Labs) were fed a normal rat diet with free access to water. Rats were randomly allocated into 3 groups: (1) control group, (2) lithium treatment group, (3) amiloride and lithium treatment group (n=8 for each group) for a duration of 6 months. Lithium carbonate (Sigma) was added to the dry food at 0.1% (0.05% of wet food, corresponding to 2,7 mmol/kg of body weight of lithium). Amiloride was added to the diet at a concentration of 200 mmol/kg of dry food, as previously described (22). Both Lithium and Amiloride were blended with wet ground food, totally solubilizing in the water used to wet the food. Food was subsequently dried to form dense kibbles. Control food underwent a similar processing method.

### *Sample processing*

Urine and plasma were collected at 4, 5 and 6 months during metabolic cage housing. Sublingual blood collection was performed under gas anesthesia, followed by centrifugation of the 500 µl blood sample with 10% heparinization at 5000 rpm. The supernatant plasma was then collected and stored at -20°C until further processing for biochemical analyses. Creatinine measurement was performed using a Konelab device (ThermoFischer Scientific). Urine osmolality was measured using the Advanced 3250 osmometer (Advances Instruments). Plasma lithium was measured by mass spectrometry (Inductively Couple Plasma Mass Spectrometry, ICP-MS, NexION 2000 spectrometer, Perkin Elmer). At the end of the protocol (6 months), after anesthesia, the left kidney was rapidly excised, partly embedded into Optimal Cutting Temperature embedding medium (OCT, Fisher Healthcare) and frozen for fluorescent immunostainings, and partly frozen and conserved at -80°C for subsequent RNA analyses. Aorta was subsequently cannulated in order to perfuse the right kidney with isotonic saline

first, and 4% paraformaldehyde (PFA) second. The right kidney was removed, fixed in 4% PFA solution, embedded in paraffin and further processed for Masson trichrome staining (3µm sections).

#### *Urine concentration tests*

Rats were monitored in metabolic cages for a duration of 24 hours each session. Water deprivation and desmopressin challenging tests were performed separately twice, after 3 and 6 months of treatment in metabolic cages. For the final timepoint (6 months), metabolic cage assessments were conducted 2 days prior to sacrifice. This timeframe was consistent for all rats. Although the assessments were spread over two days due to technical constraints, the sacrifices were scheduled accordingly, also spread over two days to ensure uniformity in the duration between the experiment and sacrifice. They respectively consisted in a 6-hour hydric restriction with urine collection at 2, 4 and 6 hours and in an intramuscular injection of desmopressin (DDAVP) (0.75 µM/kg) after 2 hours of hydric restriction, with subsequent urine collection at 2 and 4 hours after injection.

#### *Immunofluorescent assay*

Snap-frozen kidney samples were processed after cryosection (4µm sections) for immunofluorescence microscopy using a two-step staining, the first step with primary antibodies (goat anti-AQP2 SC-9882, 1/500, Santa Cruz, rabbit anti-AE1 20112, 1/800, Cell Signaling), and secondary antibodies (donkey anti-goat AF488, SC-362255, Santa Cruz, donkey anti-rabbit AF555 A-31572, 1/500, ThermoFischer Scientific), the second step with direct FITC-labeled Ki67 antibody specific for Ki67 (1/500; Abcam ab281847).

#### *Morphometric analyses*

Whole sagittal sections of kidneys were scanned using Axioscan Z1 slide scanner (Zeiss) after Masson trichrome staining or immunofluorescent labeling. Tubular area was semi-automatically measured using the QuPath software (46). Briefly, approximately one sixth of

the cortex was selected on Masson-stained tissue slices, and vessels (arteries and veins) were manually excluded. A pixel classification method was trained from manual annotations, in order to differentiate tubular lumen and parenchyma. A cut-off of 1500  $\mu\text{m}^2$  was then applied on 'lumen' objects in order to exclude glomerulus urinary spaces and peritubular capillaries. An average of  $436 \pm 223$  tubules were analyzed in each kidney (including all the tubules present within the renal cortex).

The ratio between principal cells (stained with AQP2) and type A intercalated cells (stained with AE1, type 1 anion-exchanger), and between the number of cells and the tubular area was assessed in dilated-microcystic and non-dilated hypertrophied collecting ducts. Only cells with visible nucleus were counted, and all the tubules displayed closed lumen.

#### *RT-PCR*

Kidney samples were separated immediately after excision to obtain specific samples from the cortex, the outer stripe of the outer medulla, the inner stripe of the outer medulla, and the inner medulla (including the papilla). Total RNA was extracted from these samples using the RNeasy Micro-Kit according to the manufacturer's protocol (Qiagen). Reverse transcription was performed using first-strand cDNA synthesis kit for RT-PCR (Roche Diagnostics). qPCR was then performed on a LightCycler (Roche Diagnostics) using a SYBR green kit (LightCycler 480 SYBR Green Master, Roche Diagnostics) for AQP2 (forward primer: 5'- ACC TGG CTG TCA ATG CTC TC - 3' and reverse primer: 3'- GG ACG GGA GAG GTA ACC AAA - 5'), and Pendrin (forward primer: 5'- ACT GGA ACT CTG AAC TCC CG - 3' and reverse primer: 3'- CAAAGAACCCACACTGCTCC - 5') normalizing to the ribosomal protein S23 (RPS23) transcript levels (forward primer: CTC ACG CAA AGG GAA TTG T..., reverse primer: CAA TGA AGT TCA AGC AAC CG...).

#### *Statistical analyses*

All data are presented as percentages or mean  $\pm$  SEM values. As the parameters did not display normal distribution, nNon-parametric Mann-Whitney or Kruskal-Wallis tests were

performed to test differences between groups. Non-parametric Spearman test was used to test correlations between AQP2 expression and the cellular quantifications. The significance level of a statistical hypothesis test was set at 0.05. All statistical analyses and graphs were performed using Prism GraphPad.

**Author Contributions:** Conceptualization, BM, NT, LC; methodology, BM, NT, LC, MT, MK; software, NT, MT, CK; validation, NT, MK, MT, JP, PH, CK, LC, GC, SL, LC, BM; formal analysis, MT, NT; investigation, NT, MK, MT, JP, PH, CK, LC, GC, SL, LC, BM; resources, NT, MK, MT, JP, PH, CK, LC, GC, SL, LC, BM; data curation, MK, NT, MT; writing—original draft preparation, NT; writing—review and editing, NT, MK, MT, JP, PH, CK, LC, GC, SL, LC, BM; visualization, NT, MK, MT, JP, PH, CK, LC, GC, SL, LC, BM; supervision, NT, LC, BM; project administration, BM; funding acquisition, NT. All authors have read and agreed to the published version of the manuscript.

**Funding:** This research was funded by Agence Nationale de Recherche (ANR), project ANR-21-CE14-0040-01 (GC), 22-CE14-0077-01 (NT), and the Société Francophone de Néphrologie, Dialyse et Néphrologie (RAK22005DDA, NT).

**Institutional Review Board Statement:** The animal study protocol was approved by the Ethics committee of Université Paris Cité and by the French Ministry of Research (approval # 26674-2020020714451509).

## References

1. Geddes JR, Burgess S, Hawton K, Jamison K, Goodwin GM. Long-term lithium therapy for bipolar disorder: systematic review and meta-analysis of randomized controlled trials. *Am J Psychiatry*. 2004 Feb;161(2):217–22.
2. BALANCE investigators and collaborators, Geddes JR, Goodwin GM, Rendell J, Azorin JM, Cipriani A, et al. Lithium plus valproate combination therapy versus monotherapy for relapse prevention in bipolar I disorder (BALANCE): a randomised open-label trial. *Lancet Lond Engl*. 2010 Jan 30;375(9712):385–95.
3. Miura T, Noma H, Furukawa TA, Mitsuyasu H, Tanaka S, Stockton S, et al. Comparative efficacy and tolerability of pharmacological treatments in the maintenance treatment of bipolar disorder: a systematic review and network meta-analysis. *Lancet Psychiatry*. 2014 Oct;1(5):351–9.
4. Tabibzadeh N, Vrtovsnik F, Serrano F, Vidal-Petiot E, Flamant M. [Chronic metabolic and renal disorders related to lithium salts treatment]. *Rev Med Interne*. 2019 Sep;40(9):599–608.
5. McKnight RF, Adida M, Budge K, Stockton S, Goodwin GM, Geddes JR. Lithium toxicity profile: a systematic review and meta-analysis. *Lancet Lond Engl*. 2012 Feb 25;379(9817):721–8.
6. Shine B, McKnight RF, Leaver L, Geddes JR. Long-term effects of lithium on renal, thyroid, and parathyroid function: a retrospective analysis of laboratory data. *Lancet Lond Engl*. 2015 Aug 1;386(9992):461–8.
7. Walker RJ, Leader JP, Bedford JJ, Gobe G, Davis G, Vos FE, et al. Chronic interstitial fibrosis in the rat kidney induced by long-term (6-mo) exposure to lithium. *Am J Physiol-Ren Physiol*. 2013 Feb;304(3):F300–7.
8. Kling MA, Fox JG, Johnston SM, Toloff-Rubin NE, Rubin RH, Colvin RB. Effects of long-term lithium administration on renal structure and function in rats. A distinctive tubular lesion. *Lab Invest J Tech Methods Pathol*. 1984 May;50(5):526–35.
9. Hestbech J, Hansen HE, Amdisen A, Olsen S. Chronic renal lesions following long-term treatment with lithium. *Kidney Int*. 1977 Sep;12(3):205–13.
10. Christensen S, Ottosen PD. Lithium-induced uremia in rats - a new model of chronic renal failure. *Pflugers Arch*. 1983 Nov;399(3):208–12.
11. Markowitz GS, Radhakrishnan J, Kambham N, Valeri AM, Hines WH, D'agati VD. Lithium Nephrotoxicity A Progressive Combined Glomerular and Tubulointerstitial Nephropathy. *J Am Soc Nephrol*. 2000 Jan 8;11(8):1439–48.
12. Christensen BM, Marples D, Kim YH, Wang W, Frøkiaer J, Nielsen S. Changes in cellular composition of kidney collecting duct cells in rats with lithium-induced NDI. *Am J Physiol Cell Physiol*. 2004 Apr;286(4):C952-964.
13. de Groot T, Alsady M, Jaklofsky M, Otte-Höller I, Baumgarten R, Giles RH, et al. Lithium causes G2 arrest of renal principal cells. *J Am Soc Nephrol JASN*. 2014 Mar;25(3):501–10.
14. Nielsen J, Hoffert JD, Knepper MA, Agre P, Nielsen S, Fenton RA. Proteomic analysis of lithium-induced nephrogenic diabetes insipidus: mechanisms for aquaporin 2 down-

- regulation and cellular proliferation. *Proc Natl Acad Sci U S A*. 2008 Mar 4;105(9):3634–9.
15. Alsady M, Baumgarten R, Deen PMT, Groot T de. Lithium in the Kidney: Friend and Foe? *J Am Soc Nephrol*. 2016 Jun 1;27(6):1587–95.
  16. Walker RJ, Weggery S, Bedford JJ, McDonald FJ, Ellis G, Leader JP. Lithium-induced reduction in urinary concentrating ability and urinary aquaporin 2 (AQP2) excretion in healthy volunteers. *Kidney Int*. 2005 Jan;67(1):291–4.
  17. Davis J, Desmond M, Berk M. Lithium and nephrotoxicity: a literature review of approaches to clinical management and risk stratification. *BMC Nephrol*. 2018 Nov 3;19(1):305.
  18. Tabibzadeh N, Vidal-Petiot E, Cheddani L, Haymann JP, Lefevre G, Etain B, et al. Chronic Lithium Therapy and Urine-Concentrating Ability in Individuals With Bipolar Disorder: Association Between Daily Dose and Resistance to Vasopressin and Polyuria. *Kidney Int Rep*. 2022 Jul;7(7):1557–64.
  19. Tabibzadeh N, Faucon AL, Vidal-Petiot E, Serrano F, Males L, Fernandez P, et al. Determinants of Kidney Function and Accuracy of Kidney Microcysts Detection in Patients Treated With Lithium Salts for Bipolar Disorder. *Front Pharmacol*. 2021;12:784298.
  20. Batlle DC, von Rott AB, Gaviria M, Grupp M. Amelioration of Polyuria by Amiloride in Patients Receiving Long-Term Lithium Therapy. *N Engl J Med*. 1985 Feb 14;312(7):408–14.
  21. Bedford JJ, Weggery S, Ellis G, McDonald FJ, Joyce PR, Leader JP, et al. Lithium-induced Nephrogenic Diabetes Insipidus: Renal Effects of Amiloride. *Clin J Am Soc Nephrol*. 2008 Jan 9;3(5):1324–31.
  22. Kortenoeven MLA, Li Y, Shaw S, Gaeggeler HP, Rossier BC, Wetzels JFM, et al. Amiloride blocks lithium entry through the sodium channel thereby attenuating the resultant nephrogenic diabetes insipidus. *Kidney Int*. 2009 Jul;76(1):44–53.
  23. Tabibzadeh N, Crambert G. Mechanistic insights into the primary and secondary alterations of renal ion and water transport in the distal nephron. *J Intern Med*. 2022 Jul 31;
  24. Christensen BM, Zuber AM, Loffing J, Stehle JC, Deen PMT, Rossier BC, et al.  $\alpha$ ENaC-mediated lithium absorption promotes nephrogenic diabetes insipidus. *J Am Soc Nephrol JASN*. 2011 Feb;22(2):253–61.
  25. Kalita-De Croft P, Bedford JJ, Leader JP, Walker RJ. Amiloride modifies the progression of lithium-induced renal interstitial fibrosis. *Nephrology*. 2018;23(1):20–30.
  26. Mehta PM, Gimenez G, Walker RJ, Slatter TL. Reduction of lithium induced interstitial fibrosis on co-administration with amiloride. *Sci Rep*. 2022 Aug 26;12(1):14598.
  27. Himmel NJ, Wang Y, Rodriguez DA, Sun MA, Blount MA. Chronic lithium treatment induces novel patterns of pendrin localization and expression. *Am J Physiol-Ren Physiol*. 2018 Aug;315(2):F313–22.
  28. Wall SM, Hassell KA, Royaux IE, Green ED, Chang JY, Shipley GL, et al. Localization of pendrin in mouse kidney. *Am J Physiol Renal Physiol*. 2003 Jan;284(1):F229–241.
  29. Nolen WA, Licht RW, Young AH, Malhi GS, Tohen M, Vieta E, et al. What is the optimal serum level for lithium in the maintenance treatment of bipolar disorder? A systematic review and recommendations from the ISBD/IGSLI Task Force on treatment with

lithium. *Bipolar Disord.* 2019 Aug;21(5):394–409.

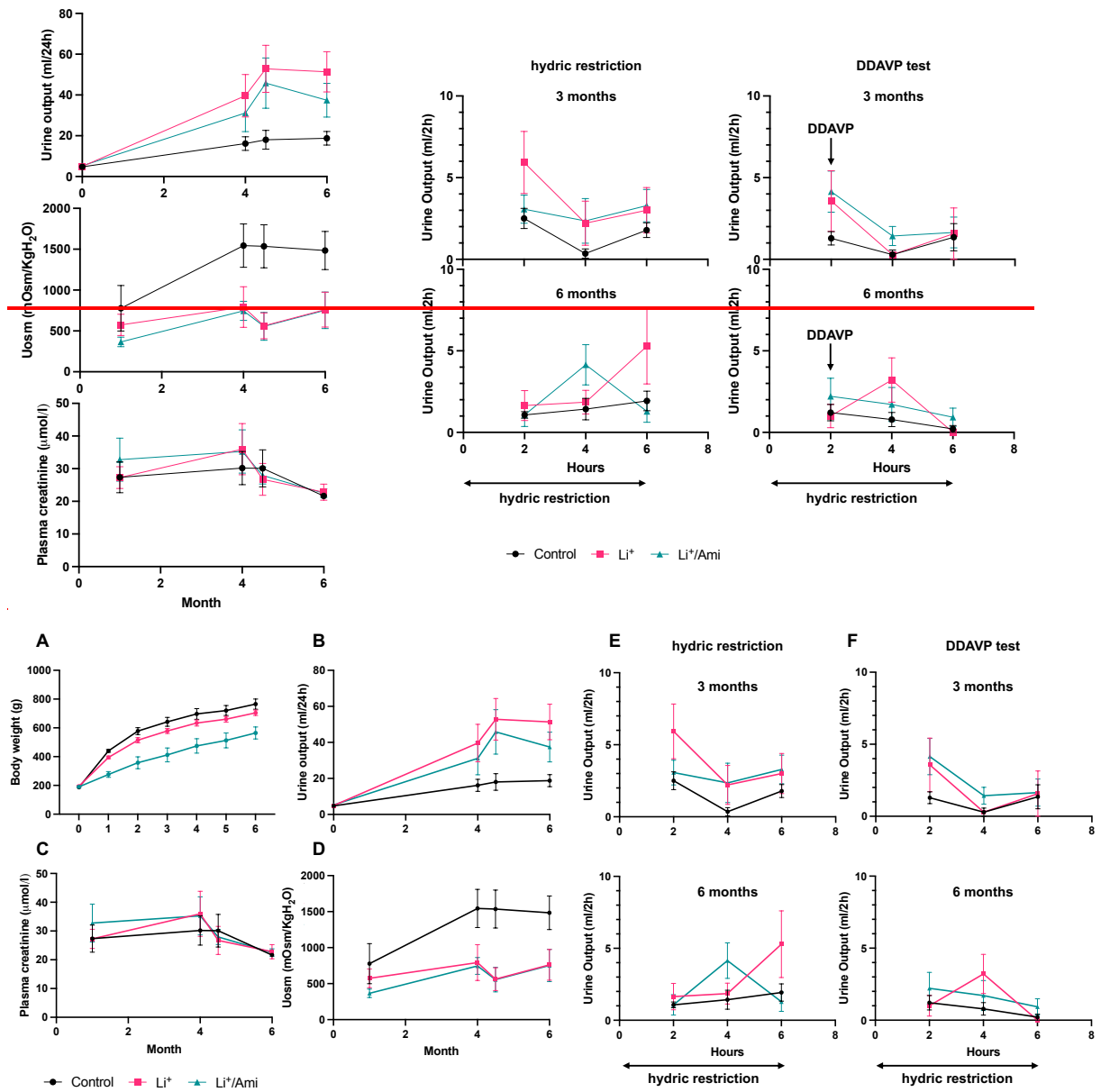
30. Bissler JJ, Zadjali F, Bridges D, Astrinidis A, Barone S, Yao Y, et al. Tuberous sclerosis complex exhibits a new renal cystogenic mechanism. *Physiol Rep.* 2019 Jan;7(2):e13983.
31. Barone S, Zahedi K, Brooks M, Henske EP, Yang Y, Zhang E, et al. Kidney intercalated cells and the transcription factor FOXi1 drive cystogenesis in tuberous sclerosis complex. *Proc Natl Acad Sci U S A.* 2021 Feb 9;118(6):e2020190118.
32. Sullivan LP, Wallace DP, Grantham JJ. Epithelial transport in polycystic kidney disease. *Physiol Rev.* 1998 Oct;78(4):1165–91.
33. de Lemos Barbosa CM, Souza-Menezes J, Amaral AG, Onuchic LF, Cebotaru L, Guggino WB, et al. Regulation of CFTR Expression and Arginine Vasopressin Activity Are Dependent on Polycystin-1 in Kidney-Derived Cells. *Cell Physiol Biochem Int J Exp Cell Physiol Biochem Pharmacol.* 2016;38(1):28–39.
34. McConnachie DJ, Stow JL, Mallett AJ. Ciliopathies and the Kidney: A Review. *Am J Kidney Dis Off J Natl Kidney Found.* 2021 Mar;77(3):410–9.
35. Park J, Shrestha R, Qiu C, Kondo A, Huang S, Werth M, et al. Single-cell transcriptomics of the mouse kidney reveals potential cellular targets of kidney disease. *Science.* 2018 May 18;360(6390):758–63.
36. Trepiccione F, Capasso G, Nielsen S, Christensen BM. Evaluation of cellular plasticity in the collecting duct during recovery from lithium-induced nephrogenic diabetes insipidus. *Am J Physiol Renal Physiol.* 2013 Sep 15;305(6):F919-929.
37. Christensen BM, Kim YH, Kwon TH, Nielsen S. Lithium treatment induces a marked proliferation of primarily principal cells in rat kidney inner medullary collecting duct. *Am J Physiol-Ren Physiol.* 2006 Jul 1;291(1):F39–48.
38. Mukherjee M, deRiso J, Otterpohl K, Ratnayake I, Kota D, Ahrenkiel P, et al. Endogenous Notch Signaling in Adult Kidneys Maintains Segment-Specific Epithelial Cell Types of the Distal Tubules and Collecting Ducts to Ensure Water Homeostasis. *J Am Soc Nephrol.* 2019 Jan 1;30(1):110–26.
39. Beunon P, Barat M, Dohan A, Cheddani L, Males L, Fernandez P, et al. MRI based Kidney Radiomics analysis during chronic lithium treatment. *Eur J Clin Invest.* 2022 Feb 1;e13756.
40. Harris PJ. Stimulation of proximal tubular sodium reabsorption by ile5 angiotensin II in the rat kidney. *Pflugers Arch.* 1979 Jul;381(1):83–5.
41. Bedford JJ, Leader JP, Jing R, Walker LJ, Klein JD, Sands JM, et al. Amiloride restores renal medullary osmolytes in lithium-induced nephrogenic diabetes insipidus. *Am J Physiol-Ren Physiol.* 2008 Apr 1;294(4):F812–20.
42. Cheval L, Viollet B, Klein C, Rafael C, Figueres L, Devevre E, et al. Acidosis-induced activation of distal nephron principal cells triggers Gdf15 secretion and adaptive proliferation of intercalated cells. *Acta Physiol Oxf Engl.* 2021 Jul;232(3):e13661.
43. Gueutin V, Vallet M, Jayat M, Peti-Peterdi J, Cornière N, Leviel F, et al. Renal  $\beta$ -intercalated cells maintain body fluid and electrolyte balance. *J Clin Invest.* 2013 Oct;123(10):4219–31.



44. Kleyman TR, Satlin LM, Hallows KR. Opening lines of communication in the distal nephron. *J Clin Invest.* 2013 Oct;123(10):4139–41.
45. Sung CC, Chen L, Limbutara K, Jung HJ, Gilmer GG, Yang CR, et al. RNA-Seq and protein mass spectrometry in microdissected kidney tubules reveal signaling processes initiating lithium-induced nephrogenic diabetes insipidus. *Kidney Int.* 2019 Aug;96(2):363–77.
46. Bankhead P, Loughrey MB, Fernández JA, Dombrowski Y, McArt DG, Dunne PD, et al. QuPath: Open source software for digital pathology image analysis. *Sci Rep.* 2017 Dec 4;7(1):16878.

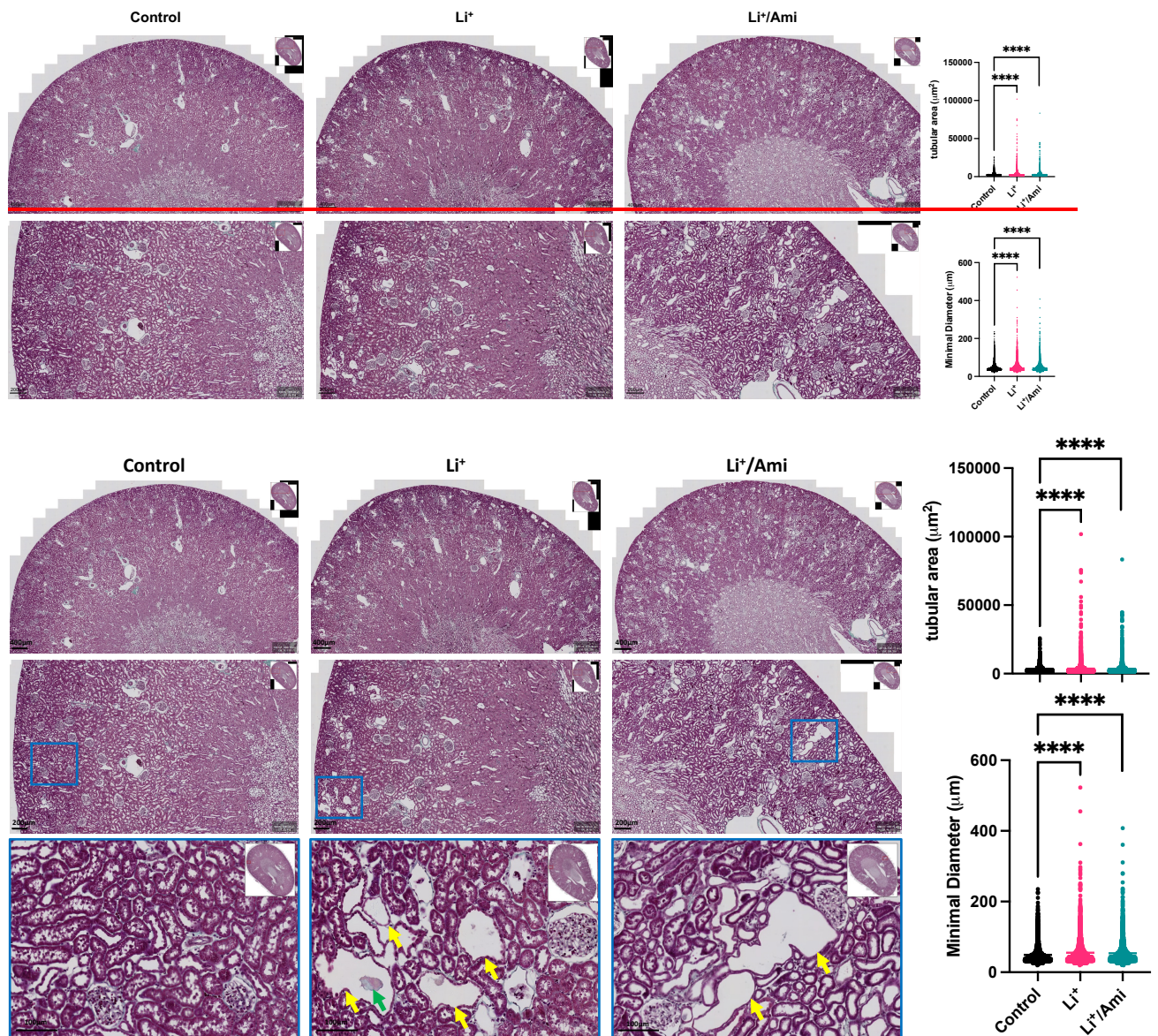
## Figures

Figure 1. Weight, uUrine concentration and plasma creatinine levels.



Data are expressed in mean and SEM. Uosm: urine osmolality, Li<sup>+</sup>: lithium, Li<sup>+</sup>/Ami: lithium and amiloride treatment. Weight gain was significantly lower in the Li<sup>+</sup>/Ami group. There were no other statistically significant difference between the groups in all the analyses.

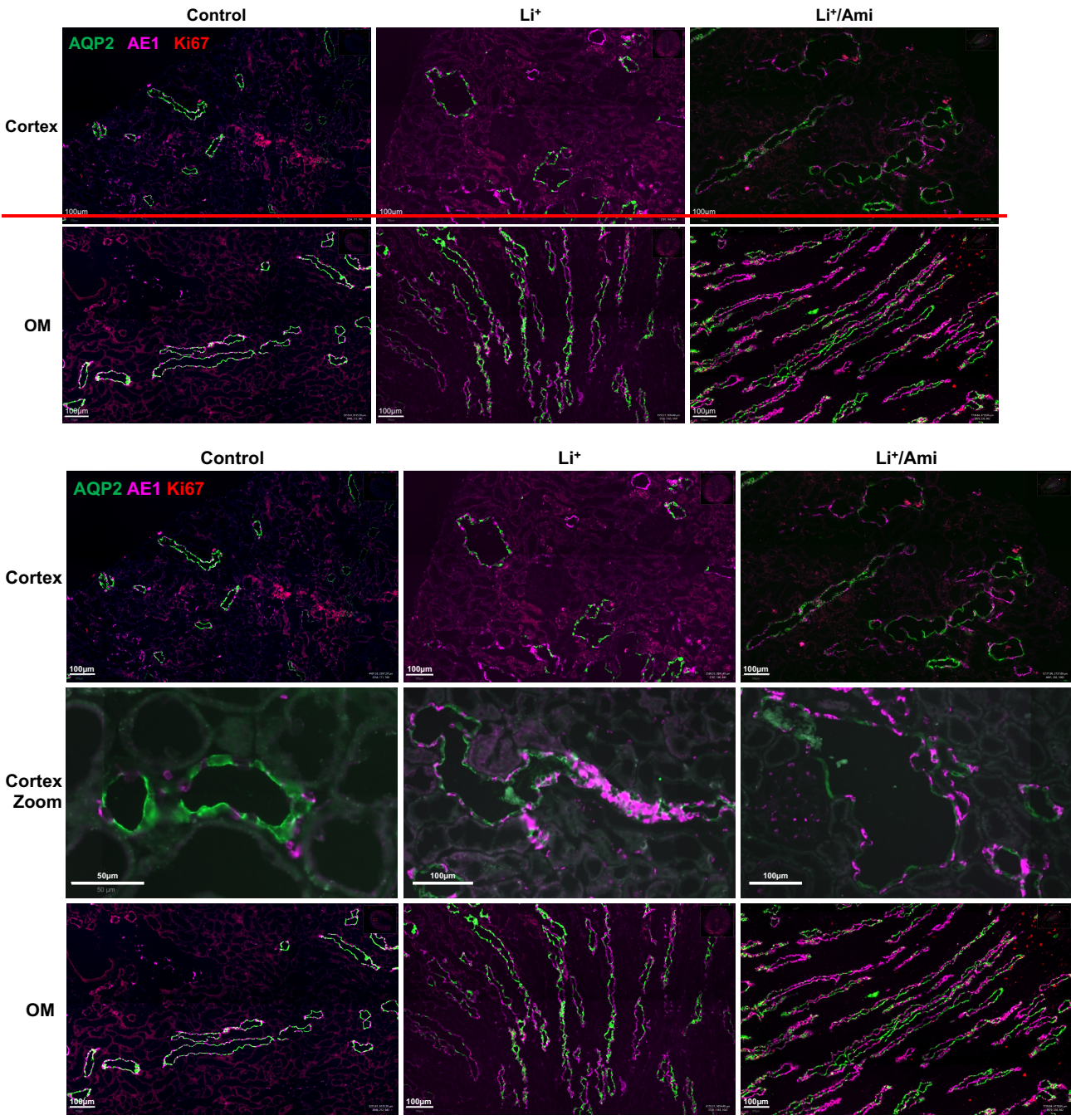
**Figure 2. Masson's trichrome staining of kidneys and quantification of tubular areas and minimal tubular diameters.**



Representative images of trichrome staining (left) with zoomed-in images showing microcystic tubular structures (yellow arrows) in the  $\text{Li}^+$  and the  $\text{Li}^+/\text{Ami}$  group, sometimes enclosing tubular casts (green arrow). Automated tubular areas and minimal diameters in each group (right). Only statistically significant differences are represented. \*\*\*\*  $p < 0.0001$ . Uosm: urine osmolality,  $\text{Li}^+$ : lithium,  $\text{Li}^+/\text{Ami}$ : lithium and amiloride treatment.

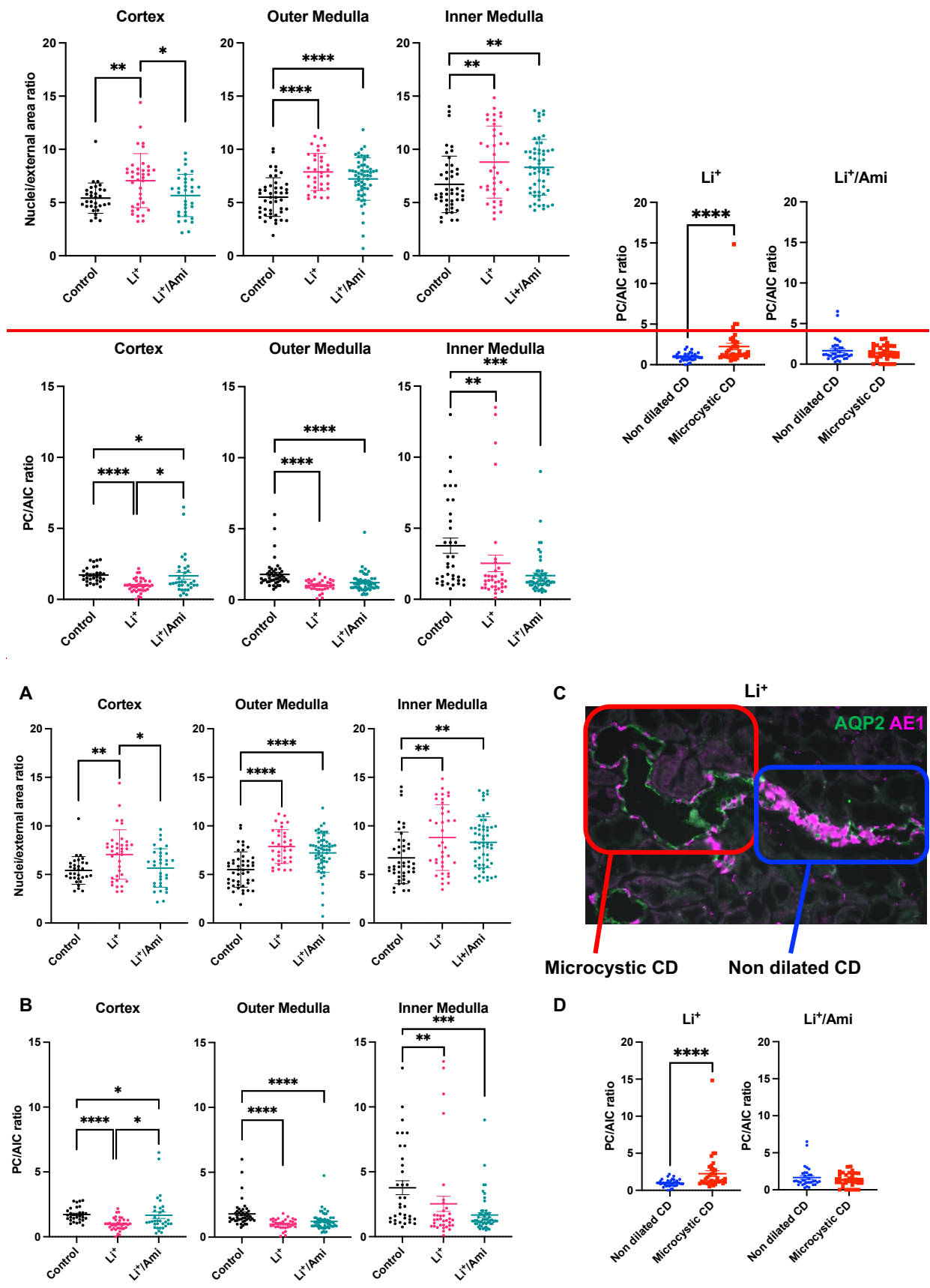


**Figure 3. Immunofluorescent staining of collecting duct cells**



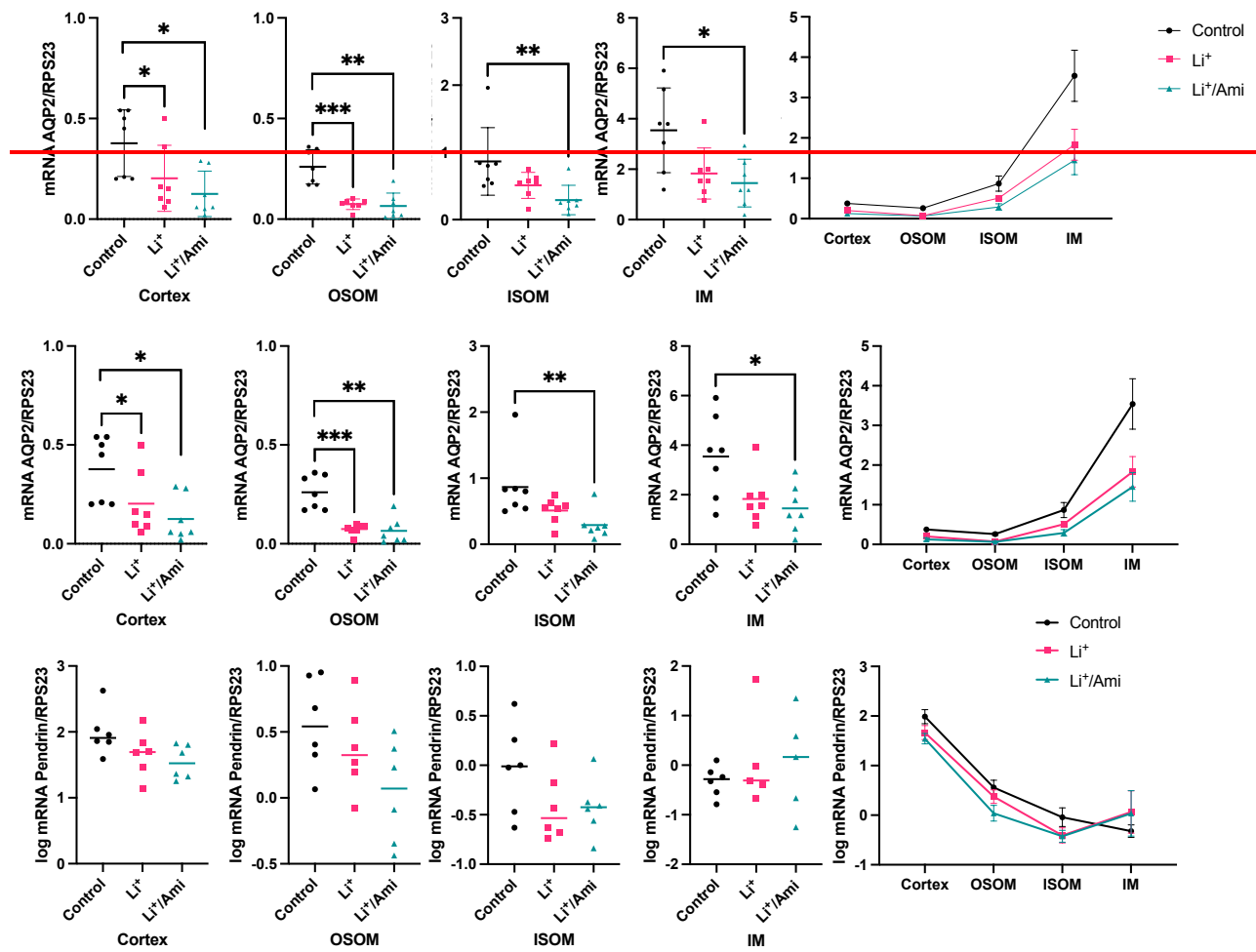
Representative images of the cortex and the outer medulla (OM) of immunofluorescent staining of type 2 aquaporin (AQP2), type 1 anion exchanger (AE1) and Ki67 of kidney slices of control rats, rats treated with lithium (Li<sup>+</sup>) and rats treated with lithium and amiloride (Li<sup>+</sup>/Ami). No collecting duct cells stained positive for Ki67.

**Figure 4. Morphometric analyses and cellular composition of collecting ducts**



Upper panel A, ratio between the numbers of DAPI-stained nuclei and external surface measurement of the collecting ducts in the cortex, the outer medulla and the inner medulla of control rats, rats treated with lithium (Li<sup>+</sup>), and with lithium and amiloride (Li<sup>+</sup>/Ami). Lower panel B, ratio between principal cells (PC) and type A intercalated cells (AIC) in the cortex, the outer medulla and the inner medulla of control rats, rats treated with lithium (Li<sup>+</sup>) and rats treated with lithium and amiloride (Li<sup>+</sup>/Ami). Right panel C, representative image of a longitudinal section of a collecting duct in the Li<sup>+</sup> group, showing a microcystic portion delineated by a majority of AQP2+ cells, and a consecutive portion with minimal lumen (non-dilated) delineated by a majority of AE1+ cells. This aspect was observed only in the Li<sup>+</sup> and the Li<sup>+</sup>/Ami groups. D, ratio between principal cells (PC) and type A intercalated cells (AIC) in the cortex of rats treated with lithium (Li<sup>+</sup>) and rats treated with lithium and amiloride (Li<sup>+</sup>/Ami) in non-dilated (hypertrophied) and in dilated (microcystic) collecting ducts (CD). \*p<0.05, \*\*p<0.01, \*\*\*p<0.001, \*\*\*\*p<0.0001.

**Figure 5. AQP2 expression in the different segments of the kidney**



Upper panel, rRelative AQP2 mRNA expression in the cortex, the outer stripe of the outer medulla (OSOM), the inner stripe of the inner medulla (ISOM) and the inner medulla (IM) in control rats, rats treated with lithium (Li<sup>+</sup>) and rats treated with lithium and amiloride (Li<sup>+</sup>/Ami). Lower panel, relative Pendrin log mRNA expression in the cortex, the outer stripe of the outer medulla (OSOM), the inner stripe of the inner medulla (ISOM) and the inner medulla (IM) in control rats, rats treated with lithium (Li<sup>+</sup>) and rats treated with lithium and amiloride (Li<sup>+</sup>/Ami). \* p<0.05, \*\* p<0.01, \*\*\* p<0.001. RPS23: ribosomal protein S23.

## **Graphical abstract**

Lithium treatment is the main treatment of bipolar disorder but can induce renal adverse events, including nephrogenic diabetes insipidus (NDI) and microcystic chronic kidney disease (CKD). We found that in a long-term treatment rat model, low exposition to lithium prevented NDI, but not microcysts, which were predominantly composed of collecting ducts principal cells, conversely to hypertrophic zones of the collecting duct that were mainly bordered by intercalated cells.



